Stress Wave Propagation in Larch Plantation Trees—Numerical Simulation

Fenglu Liu
School of Technology, Beijing Forestry University, Beijing, China, liufenglu39@126.com

Fang Jiang
School of Technology, Beijing Forestry University, Beijing, China, jf0602@bjfu.edu.cn

Xiping Wang
USDA Forest Service Forest Products Laboratory, Madison, Wisconsin, USA, xwang@fs.fed.us

Houjiang Zhang
School of Technology, Beijing Forestry University, Beijing, China, hjzhang6@bjfu.edu.cn

Wenhua Yu
School of Technology, Beijing Forestry University, Beijing, China, yuwenhua56@sina.com

Abstract

In this paper, we attempted to simulate stress wave propagation in virtual tree trunks and construct two dimensional (2D) wave-front maps in the longitudinal-radial section of the trunk. A tree trunk was modeled as an orthotropic cylinder in which wood properties along the fiber and in each of the two perpendicular directions were different. We used the COMSOL Multiphysics® software to conduct numerical simulations. Field stress wave timing measurements were then conducted on three freshly cut larch (*Larix principis-rupprechtii* Mayr) logs to validate the simulation results. The 2D wave fronts observed through numerical simulations were in good agreement with those obtained through stress wave timing measurements. When a stress wave was introduced into the tree trunk through a point impact, it initially propagated in the impact direction with a spherical wave front; then the flow of stress wave energy gradually changed toward the longitudinal direction and its wave front became flattened perpendicular to the longitudinal axis. Our preliminary results indicate that the Structural Mechanics module of the COMSOL Multiphysics® software is capable of simulating the longitudinal wave propagation in standing trees.

Keywords: longitudinal stress wave, logs, standing trees, numerical simulation, time-of-flight, wave front.

Introduction

The use of stress wave technology for standing tree quality assessment has received a lot of attention in recent years (Carter et al. 2005, Chauhan and Walker 2006, Grabianowski et al. 2006, Wang et al. 2007a, Raymond et al. 2008, Mora et al. 2009, Mahon et al. 2009). By far, most research has been limited to direct measurement of stress wave velocity in trees. Subsequent wood property prediction was solely based on the measured velocity values (Addis et al. 2000, Huang 2000, Wang et al. 2001, Lindstrom et al. 2002, Wang et al. 2007b). A typical approach for measuring stress wave velocity in trees involves inserting two sensor probes (transmit probe and receiver probe) into the sapwood and introducing a stress wave impulse into the tree trunk from a mechanical impact (Wang et al. 2007a, b). The standing tree device essentially measures the time for the stress wave to travel from the transmit probe to the receiver probe. The stress wave velocity is subsequently calculated from the span between two sensor probes and the time of flight (TOF) data.

Although acoustic velocity has been proven to be an effective measure for predicting wood and fiber properties in standing trees, there is still a lack of understanding of how stress waves propagate in standing trees and how tree diameter, species, tree age, and environmental conditions affect wave propagation in a tree. Zhang et al. (2011) conducted stress wave timing measurements on red pine (*Pinus resinosa* Ait.) logs to obtain stress wave data needed for simulating stress wave propagation in standing trees. With the TOF data collected from a series of cross sections along the logs, they were able to construct two dimensional (2D) and three dimensional (3D) stress wave contour maps using a commercial software. Those stress wave contour maps represent the wave fronts in a time sequence, illustrating the flow of stress wave energy within a tree trunk. Although this experimental approach provides a way to study stress wave behavior in standing trees, the procedure requires cutting down trees and the TOF measurements are time consuming.

In this paper, we attempted to simulate stress wave propagation in virtual tree trunks and construct two dimensional wave front maps in the longitudinal-radial section of the trunk. We used a COMSOL Multiphysics® (Burlington, MA) software to conduct the numerical simulations. COMSOL Multiphysics® is a finite element analysis, solver, and simulation software package that is suited for various physics and engineering applications. It has been widely used in the areas of acoustics, biological science, structural mechanics and wave propagation (Zhou et al. 2015). Our goal was to prove the validity of using the COMSOL Multiphysics® software to simulate stress wave propagation in standing timber and pave the way for further investigation of stress wave behavior in plantation trees.

Fundamentals of Wave Propagation in Wood

When stress is applied suddenly to the surface of wood, the disturbance that is generated travels through the wood as stress waves. In general, three types of waves are initiated by such an impact: (1) longitudinal wave (compressive or P-wave), (2) shear wave (S-wave), and (3) surface wave (Rayleigh wave). A longitudinal wave corresponds to the oscillation of particles along the direction of wave propagation such that particle velocity is parallel to wave velocity. In a shear wave, the motion of the particles conveying the wave is perpendicular to the direction of the propagation of the wave itself. A Rayleigh (surface) wave is usually restricted to the region adjacent to the surface; particles move both up and down and back and forth, tracing elliptical paths. Although most energy resulting from an impact is carried by shear and surface waves, the longitudinal wave travels the fastest and is the easiest to detect in field applications (Meyers 1994). Consequently, the longitudinal wave is by far the most commonly used wave for material property characterization. A basic understanding of the relationship between wood properties and longitudinal wave velocity (hereafter referred to as wave velocity) can be acquired from fundamental wave theory.

One-dimensional stress wave theory

In a long, slender, isotropic material, strain and inertia in the transverse direction can be neglected and longitudinal waves propagate in a plane waveform (wave front). The free longitudinal motion for one-dimensional wave is governed by the following partial differential equation:

$$\frac{\partial^2 u}{\partial t^2} = \frac{E}{\rho}\frac{\partial^2 u}{\partial x^2} \tag{1}$$

Where u is the longitudinal displacement, E is longitudinal modulus of elasticity, and ρ is mass density of material. In this case, the wave velocity (C_0) is independent of Poisson's ratio and is given by the following equation:

$$C_0 = \sqrt{\frac{E}{\rho}} \tag{2}$$

Three-dimensional stress wave theory

In an infinite or unbounded isotropic elastic medium, a triaxial state of stress is present. The wave front of the longitudinal wave propagating through such a medium is no longer a plane. The partial differential equation that governs the three dimensional wave is as follows (Meyers 1994):

$$\frac{\partial^2 \Delta}{\partial t^2} = \frac{\lambda + 2\mu}{\rho} \nabla^2 \Delta \tag{3}$$

where λ , μ are the Lamé constants,

$$\Delta = \varepsilon_{ii} = \varepsilon_{11} + \varepsilon_{22} + \varepsilon_{33} \tag{4}$$

$$\nabla^2 = \frac{\partial^2}{\partial x_1^2} + \frac{\partial^2}{\partial x_2^2} + \frac{\partial^2}{\partial x_3^2} \tag{5}$$

From elastic theory, $\mu = \frac{E}{2(1+\nu)}$ and $\lambda = \frac{\nu E}{(1+\nu)(1-2\nu)}$, then the longitudinal velocity in unbounded medium can be determined as

$$C = \sqrt{\frac{1-\nu}{(1+\nu)(1-2\nu)} \frac{E}{\rho}} \tag{6}$$

Where ν is Poisson's ratio of the material. From Equation (6), it is clear that the wave velocity is dependent on density and two elastic parameters, modulus of elasticity (*E*) and Poisson's ratio (ν).

Numerical Simulation of Stress Wave Propagation in Standing Trees

Both Foundation Module and Structural Mechanics Module of the COMSOL Multiphysics® software were used for the task. Foundation module has main function of pre-processing, post-processing, and solving. Structural Mechanics Module is specifically for mechanical structural analysis under static or dynamic loads, including steady state, transient, quasi-static, frequency response, and pre-stressed. The Structural Mechanics module we selected is based on three-dimensional wave equations for elastic materials. Simulation of the wave propagation was achieved by solving the partial differential equations using finite element method under defined initial and boundary conditions.

Model geometry

To facilitate the comparison of simulation results and the field experimental results, we specifically set the longitudinal–radial sections of the logs cut from the trees as the geometry models for numerical simulation. The sizes of those three log samples are shown in Table 1. The geometry model is basically in a tapered solid cylindrical form.

Material properties

A tree trunk was considered as an orthotropic cylinder, with the axial, radial, tangential directions as three principal axes. Twelve elastic constants of green larch were determined through laboratory experiments in a previous study (Liu et al. 2015). The wood specimens used for determining the elastic constants were cut from the same logs that were used for validation experiment. The average values of the elastic constants are shown in Table 2. The measured average density (ρ) of green larch was 838 kg/m^3.

Impulse load

Stress waves used in tree measurements are typically produced through a mechanical impact on the start transducer and this impact-induced stress wave has a very short duration. We used the following half-sine pulse function to express this impact force:

$$F(\mathrm{t}) = \begin{cases} \mathrm{Asin}(2\pi f\mathrm{t}), & t < (1/2f) \\ 0, & t \geq (1/2f) \end{cases} \tag{7}$$

Where A is the amplitude of pulse and f is the frequency.

According to the actual pulse signals collected from a hammer impact in a laboratory testing, the amplitudes of the pulse signals were about 200 N. Because the start sensor probe is typically inserted into a tree trunk in a 45-degree angle with respect to the longitudinal axis, the impact force acting on the start sensor is also in a 45-degree angle to the longitudinal axis of the trunk. Based on the principle of vector decomposition, *F(t)* can be decomposed into two orthogonal components: $F_y(t)$ and $F_z(t)$, and each component is 141.4N. According to the tested pulse force signal, the frequency of pulse was $f = 1\times10^8$ (Hz). The function graph of a single pulse force component is shown in Figure 1.

Table 1—Dimension of the larch logs

	Length (cm)	Large-end diameter (cm)	Small-end diameter (cm)
Log A	360	38	31
Log B	360	32	27
Log C	360	28	24

Table 2—Twelve elastic constants of larch wood obtained through laboratory experiments

Modulus of elasticity (MPa)		Modulus of rigidity (MPa)		Poisson's ratio μ	
E_L	4350.33	G_{RT}	523.18	μ_{LT}	0.41
E_T	1099.60	G_{LR}	460.32	μ_{LR}	0.23
E_R	1054.97	G_{LT}	412.42	μ_{TL}	0.10
				μ_{TR}	0.67
				μ_{RL}	0.08
				μ_{RT}	0.62

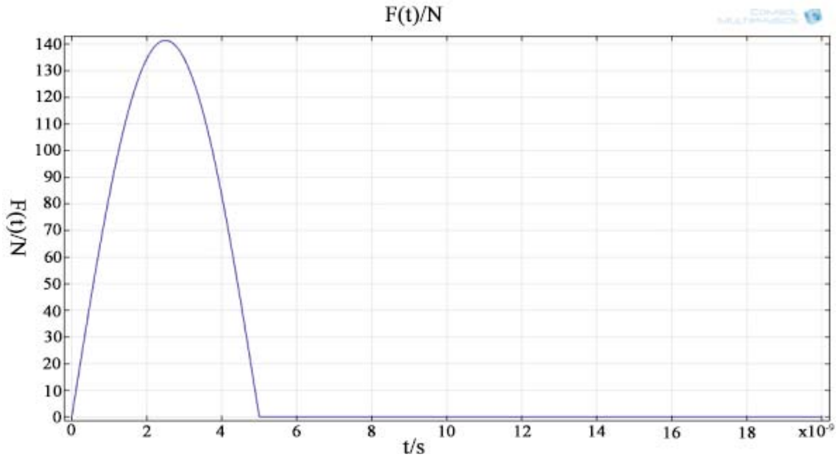

Figure 1—Function of a half-sine pulse.

Initial and boundary conditions

The initial displacement and initial velocity of each particle in wood were set as zero. u is used to represent the particle displacement, the mathematical expressions of these two initial conditions are shown below:

$$\textit{Initial displacement: } u_i = 0 \ (i = x, y, z) \tag{8}$$

$$\textit{Initial velocity: } \frac{\partial u_i}{\partial t} = 0 \ (i = x, y, z) \tag{9}$$

The virtual trunk model was set to have a free boundary condition, which means that the compression waves and reflected waves coexist with the wave attenuation when the stress wave propagates to the boundaries.

Meshing

The mesh was generated automatically with the triangular elements. Free meshing provided in COMSOL was used for the generation of mesh. The largest and smallest elements were 1.73 cm and 0.004 cm, respectively. Figure 2 shows the divided grid of longitudinal-radial section in a virtual tree trunk, which corresponds to log sample A. The mesh has been refined at the region below the excitation source. A free time step for transient solver was selected as initial step, 1e-9s; biggest step, 1e-4s. Output step of the result was 5.0e-7s. After all the settings were completed, the COMSOL program was run to obtain simulation results.

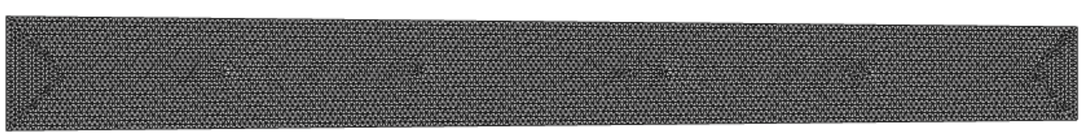

Figure 2—The geometry model of a virtual tree trunk with meshing grids.

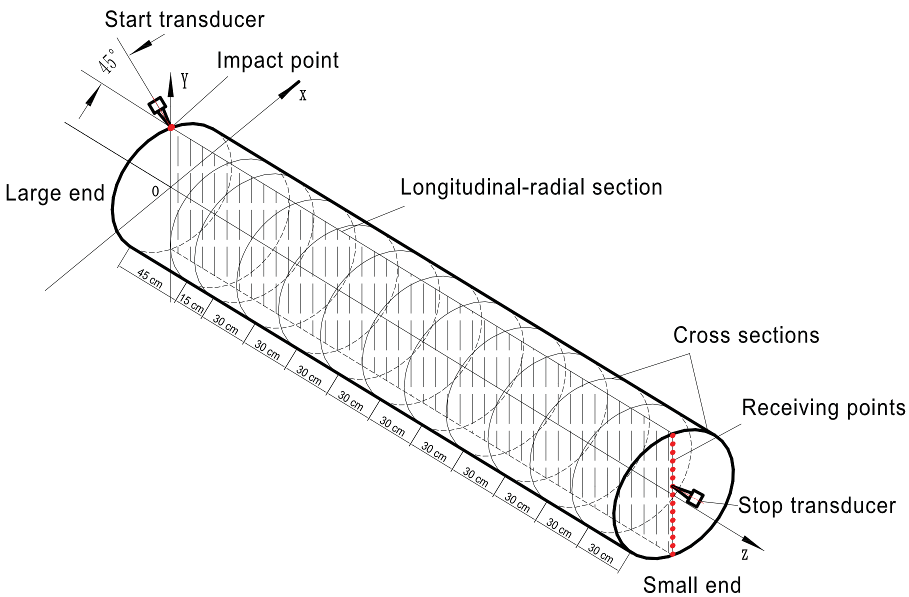

Figure 3—Schematic diagram of stress wave timing measurements on a log sample.

Experimental Validation

To validate the simulation results of stress wave propagation in standing trees, we conducted field stress wave measurements on freshly cut logs in a larch plantation stand. Three larch trees with different diameters at breast height were felled down and cut into 3.6-m long logs starting from the butt end. The first log from each tree was used to obtain stress wave data needed for developing wave front maps. Stress wave propagation time in the logs was measured using a battery-operated stress wave timer (FAKOPP Microsecond Meter, Fakopp Interprise, Hungary). Figure 3 shows the schematic diagram for conducting the field stress wave measurements.

Stress wave timing measurements were conducted when the log samples were laid flat on the ground. The start transducer was mounted on the log by inserting the spike 1-cm deep at the highest point of the large end, with an angle of 45 degrees with respect to the upper surface; while the stop transducer was mounted at the cross section of the small end by inserting the spike 1-cm deep through the end grain. The start transducer remained in the same position during the measurement process, while the position of stop transducer was continuously changed along the vertical middle lines. A constant impact on the start transducer was generated by a special pendulum device mounted onto the log. The stop transducer received stress wave signals and the time of flight (TOF) was displayed and recorded. A series of stress wave measurements were conducted by moving the stop transducer to different locations at the middle vertical lines of the end cross section. Once the stress wave measurements were completed at one end cross section, a 30-cm long section was cut off from the small end, and the same procedure was repeated on the new cross section. A total of 10 cross sections were tested for each log sample.

Results and Discussion

Contour maps of total displacement on the longitudinal-radial section were obtained through numerical simulations. The contour of displacement refers to the line in which each point has the same TOF as the stress wave propagated from the source point. As an example, Figure 4 shows the simulated results at the times of T = 5e-5s, 1e-4s, 1.4e-4s, 1.9e-4s, 2.7e-4s, 3.5e-4s, 5e-4s, 7e-4s, 9e-4s, 1e-3s. The forefront line in the contour map for each time point represents the wave front, which is the boundary of stress wave disturbance zone and undisturbed areas during the propagation.

To visually display the propagation patterns of the impact-induced stress waves in the virtual tree trunks, we extracted the forefront contour lines from the displacement contour maps at various time points to form the wave front diagram. Figure 5 shows the 2D mapping of the simulated stress wave fronts for larch virtual trunks with three different diameters, which corresponds to the three logs used in the validation experiments. The numbers next to the wave front lines are the TOF in microsecond; the red dot on the upper left of the graph is the import source; horizontal and vertical axes are the length and diameter of the tree trunk, respectively. In all three simulation cases, the wave front initially propagated in the impact direction with a spherical wave front. As the wave continuously propagated, the flow of stress wave energy gradually changed toward the longitudinal direction and its wave front gradually became flattened and close to perpendicular to the longitudinal axis.

In order to verify the accuracy and reliability of numerical simulation results, the results of simulation and the results of the field experiments are compared and analyzed. Figure 6 is a summary of the experimental results of stress wave timing measurements showing the changing patterns of the wave fronts in the longitudinal-radial section of the larch logs. Note that the stress wave timing measurements in the larch logs began at the location 45 cm from the log end, therefore the display of contour maps after post-processing is 45 cm off the log end.

When compared Figure 5 with Figure 6, it is found that stress wave propagation patterns of the numerical simulation in virtual tree trunks are basically in agreement with the results from stress wave timing measurements. We also noticed that the shape of the stress wave fronts from the field experiments was not as smooth as those from numerical simulations. Some irregular TOF contour lines occurred in the latter part of the stress wave propagation path. This might be caused by the local defects such as knots in that part of the log. Knots typical exhibit distorted grain orientations and have very different physical and mechanical properties compared with normal wood. Whereas in numerical simulations, our analysis was based on the assumption that a tree trunk is orthotropic material without any defects.

Conclusion

Stress wave propagation patterns obtained through numerical simulations were in a good agreement with the results from field stress wave measurements. When a stress wave was introduced into the tree trunk through a point impact with a 45 degree angle with respect to the trunk surface, it initially propagated in the impact direction with a spherical wave front. Then the flow of stress wave energy gradually changed towards the longitudinal direction and its wave front became flattened perpendicular to the longitudinal axis. The preliminary results of this study indicated that the orthotropic assumption for the tree trunk model for numerical simulation is reasonable. The COMSOL Multiphysics® software is capable of simulating the longitudinal wave propagation in standing trees. This opens the way to further investigate the mechanism of stress wave propagation in standing trees and examine the effects of various factors (species, tree age, tree diameter, temperature etc.) on stress wave assessment of wood quality in plantation forests.

Acknowledgment

This project was conducted under the cooperative research agreement between Beijing Forestry University, Beijing, China, and the USDA Forest Service, Forest Products Laboratory (FPL), Madison, WI. Financial support to the project was provided by the National Natural Science Foundation of China (Grant No. 31328005).

References

Addis T, Buchanan AH, Walker JCF. 2000. Selecting trees for structural timber. Holz Roh-Werkst 58:162-167.

Carter P, Briggs D, Ross RJ, Wang X. 2005. Acoustic testing to enhance western forest values and meet customer wood quality needs. PNW-GTR-642, In: Harrington, CA, Schoenholtz SH, eds. Productivity of Western Forests: A Forest Products Focus. USDA Forest Service, Pacific Northwest Research Station, Portland, Oregon. pp 121-129.

Chauhan SS, Walker JCF. 2006. Variation in acoustic velocity and density with age, and their interrelationships in radiata pine. Forest Ecol Manag 229: 388-394.

Grabianowski M, Manley B, Walker JCF. 2006. Acoustic measurements on standing trees, logs and green lumber. Wood Sci Technol 40: 205-216.

Huang CL. 2000. Predicting lumber stiffness of standing trees. In: Proceedings, the 12th International Symposium on Nondestructive Testing of Wood, University of Western Hungary, Sopron, September 13-15, 2000. Pp. 173-179.

Lindstrom H, Harris P, Nakada R. 2002. Methods for measuring stiffness of young trees. Holz Roh-Werkst 60:165-174.

Liu F; Jiang F; Zhang J ; Zhang H; Wang X; Yang Z. 2015. Study on twelve elastic constant values of larch forest. Journal of Beijing Forestry University. (in press)

Mahon JM Jr, Jordan L, Schmileck LR, Clark A III, Daniels RF. 2009. A comparison of sampling methods for a standing tree acoustic device. South J Appl For 33(2): 62-68.

Meyers MA (1994) Dynamic behavior of materials. John Wiley & Sons. Inc., New York.

Mora CR, Schimleck LR, Isik F, Mahon JM, Clark A III, Daniels RF. 2009. Relationship between acoustic varaibles and different measures of stiffness in standing *Pinus taeda* trees. Can J For Res 39:1421-1429.

Raymond CA, Joe B, Anderson DW, Watt DJ. 2008. Effect of thinning on relationships between three measures of wood stiffness in *Pinus radiata*: standing trees vs. logs vs. short clear specimens. Can. J. For. Res. 38: 2870-2879.

Wang X, Ross RJ, McClellan M, Barbour RJ, Erickson JR, Forsman JW, McGinnis GD. 2001. Nondestructive evaluation of standing trees with stress wave method. Wood Fiber Sci 33(4):522-533.

Wang X, Ross RJ, Carter P. 2007a. Acoustic evaluation of wood quality in standing trees. Part I. Acoustic wave behaviour. *Wood and Fibre Science* 39(1):28-38.

Wang X, Carter P, Ross RJ, Brashaw BK. 2007b. Acoustic assessment of wood quality of raw forest materials—a path to increased profitability. Forest Products Journal 57(5):6-14.

Zhang H, Wang X, Su J. 2011. Experimental investigation of stress wave propagation in standing trees. Holzforschung 65(5):743-748.

Zhou J, Wei C, Li W, and others. 2015. Analysis of solid elasto-plastic mechanics based on mathematical module of COMSOL Multiphysics. Engineering Journal of Wuhan University. 48(2): 195-201.

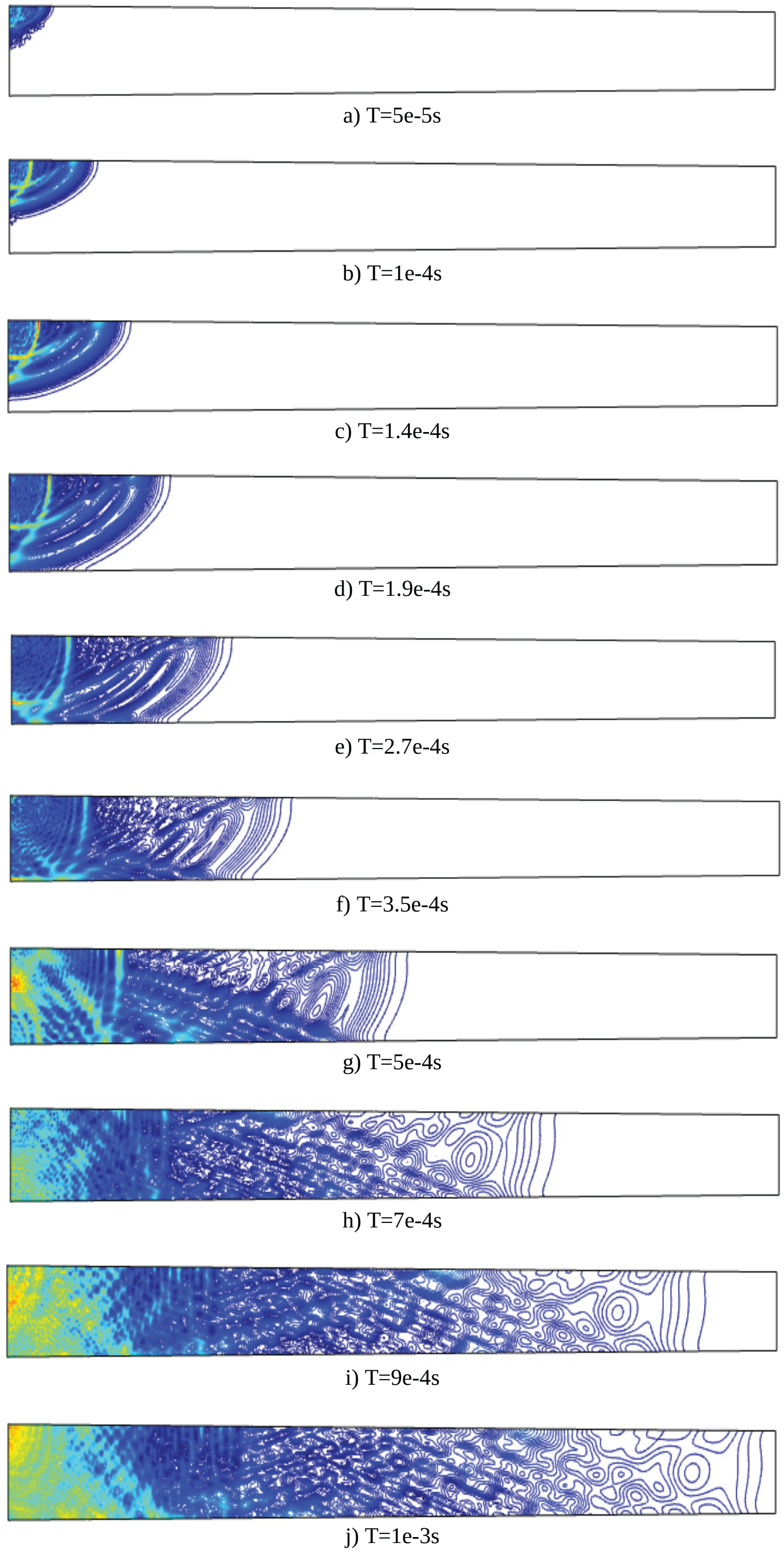

Figure 4—Contour maps of total displacement on longitudinal-radial section (log A).

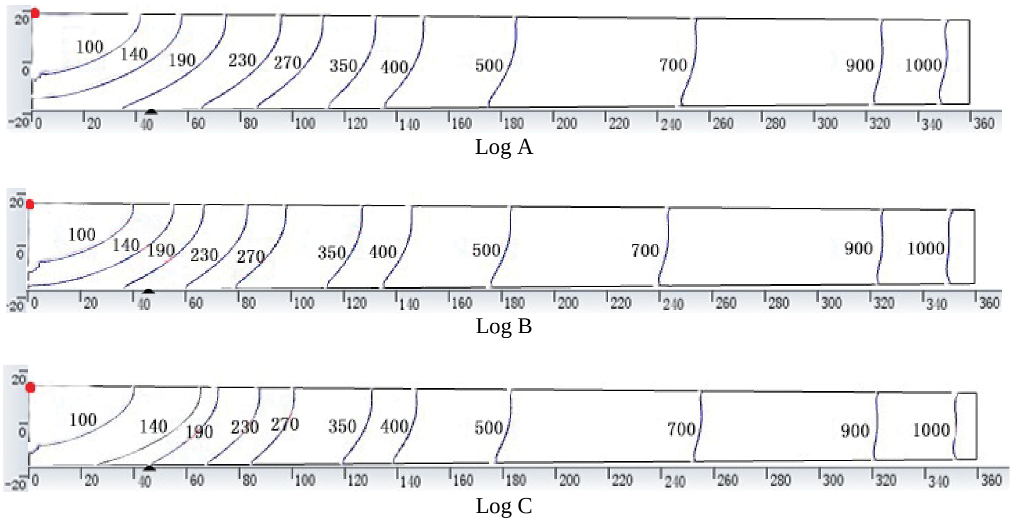

Figure 5—Wave fronts obtained through numerical simulation showing wave propagation patterns in the longitudinal-radial section of the virtual tree trunks.

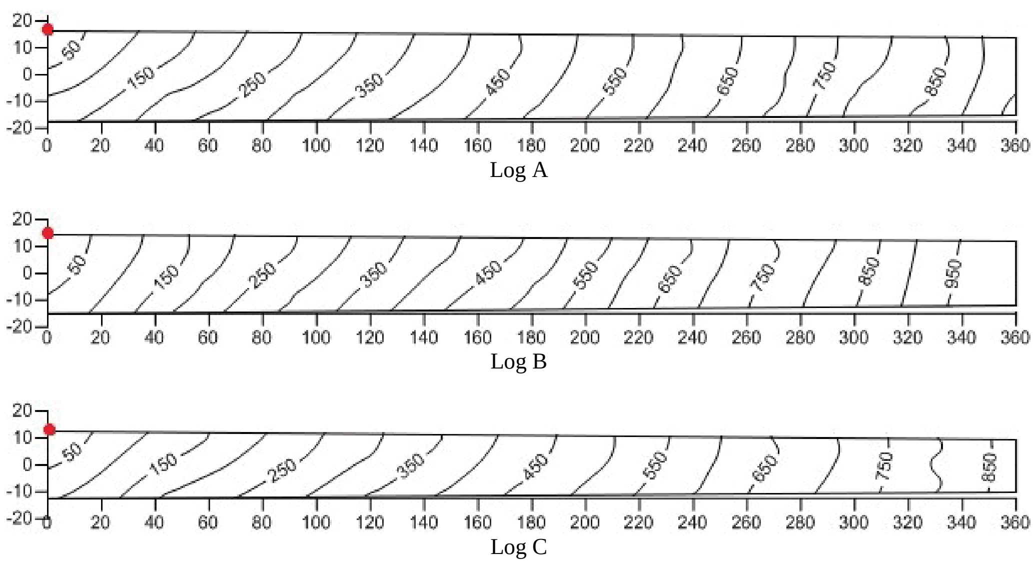

Figure 6—Experimental results of stress wave timing measurements showing the changing patterns of the wave fronts in the longitudinal-radial section of the larch logs.